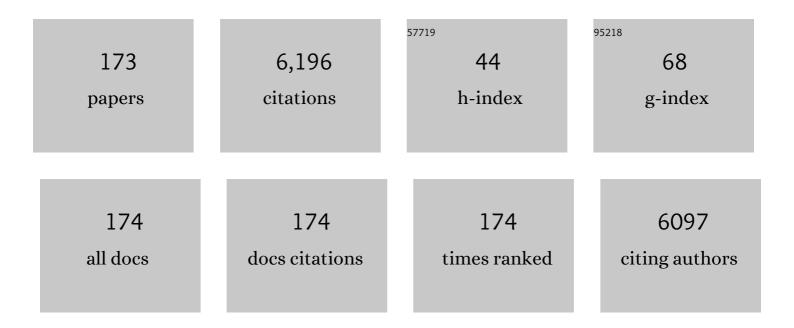
List of Publications by Year in descending order

Source: https://exaly.com/author-pdf/9110059/publications.pdf Version: 2024-02-01



YUE-DENC CAL

#	Article	IF	CITATIONS
1	Visible-Light-Driven BiOI-Based Janus Micromotor in Pure Water. Journal of the American Chemical Society, 2017, 139, 1722-1725.	6.6	283
2	One-, Two-, and Three-Dimensional Lanthanide Complexes Constructed from Pyridine-2,6-dicarboxylic Acid and Oxalic Acid Ligands. Crystal Growth and Design, 2008, 8, 4083-4091.	1.4	193
3	Cerium Based Metal–Organic Frameworks as an Efficient Separator Coating Catalyzing the Conversion of Polysulfides for High Performance Lithium–Sulfur Batteries. ACS Nano, 2019, 13, 1923-1931.	7.3	184
4	Enhanced Adsorption of <i>p</i> -Arsanilic Acid from Water by Amine-Modified UiO-67 as Examined Using Extended X-ray Absorption Fine Structure, X-ray Photoelectron Spectroscopy, and Density Functional Theory Calculations. Environmental Science & Technology, 2018, 52, 3466-3475.	4.6	148
5	Photocatalytic Micro/Nanomotors: From Construction to Applications. Accounts of Chemical Research, 2018, 51, 1940-1947.	7.6	130
6	Covalent Organic Framework Based Functional Materials: Important Catalysts for Efficient CO ₂ Utilization. Angewandte Chemie - International Edition, 2022, 61, .	7.2	128
7	3D catalytic MOF-based nanocomposite as separator coatings for high-performance Li-S battery. Chemical Engineering Journal, 2020, 381, 122701.	6.6	119
8	2-Fold Interpenetrating Bifunctional Cd-Metal–Organic Frameworks: Highly Selective Adsorption for CO ₂ and Sensitive Luminescent Sensing of Nitro Aromatic 2,4,6-Trinitrophenol. ACS Applied Materials & Interfaces, 2017, 9, 4701-4708.	4.0	113
9	Confinement of polysulfides within bi-functional metal–organic frameworks for high performance lithium–sulfur batteries. Nanoscale, 2018, 10, 2774-2780.	2.8	98
10	A Review on Artificial Micro/Nanomotors for Cancer-Targeted Delivery, Diagnosis, and Therapy. Nano-Micro Letters, 2020, 12, 11.	14.4	98
11	Construction of Three-Dimensional Metalâ^'Organic Frameworks with Helical Character through Coordinative and Supramolecular Interactions. Crystal Growth and Design, 2009, 9, 1605-1613.	1.4	97
12	A Family of Three-Dimensional Lanthanide-Zinc Heterometal–Organic Frameworks from 4,5-Imidazoledicarboxylate and Oxalate. Crystal Growth and Design, 2011, 11, 2220-2227.	1.4	92
13	Efficient Encapsulation of Small S ₂₋₄ Molecules in MOF-Derived Flowerlike Nitrogen-Doped Microporous Carbon Nanosheets for High-Performance Li–S Batteries. ACS Applied Materials & Interfaces, 2018, 10, 9435-9443.	4.0	90
14	pH-Dependent Assembly and Conversions of Six Cadmium(II)-Based Coordination Complexes. Crystal Growth and Design, 2010, 10, 3277-3284.	1.4	89
15	Construction of Metal-Imidazole-Based Dicarboxylate Networks with Topological Diversity: Thermal Stability, Gas Adsorption, and Fluorescent Emission Properties. Crystal Growth and Design, 2012, 12, 2178-2186.	1.4	87
16	Vertical Composition Distribution and Crystallinity Regulations Enable High-Performance Polymer Solar Cells with >17% Efficiency. ACS Energy Letters, 2020, 5, 3637-3646.	8.8	87
17	Single-Atom Zinc and Anionic Framework as Janus Separator Coatings for Efficient Inhibition of Lithium Dendrites and Shuttle Effect. ACS Nano, 2021, 15, 13436-13443.	7.3	87
18	Unusual Noninterpenetrating (3,6) Topological Network Assembled by Semirigid Benzimidazole-Based Bridging Ligand. Inorganic Chemistry, 2001, 40, 2210-2211.	1.9	81

YUE-PENG CAI

#	Article	IF	CITATIONS
19	Glucose-Fueled Micromotors with Highly Efficient Visible-Light Photocatalytic Propulsion. ACS Applied Materials & Interfaces, 2019, 11, 6201-6207.	4.0	79
20	Lead-Based Metal–Organic Framework with Stable Lithium Anodic Performance. Inorganic Chemistry, 2017, 56, 4289-4295.	1.9	78
21	Lithium-Ion-Battery Anode Materials with Improved Capacity from a Metal–Organic Framework. Inorganic Chemistry, 2016, 55, 8244-8247.	1.9	76
22	MOF-derived Ni ₃ S ₄ Encapsulated in 3D Conductive Network for High-Performance Supercapacitor. Inorganic Chemistry, 2020, 59, 2406-2412.	1.9	75
23	Single-Crystal-to-Single-Crystal Transformation in a One-Dimensional Agâ``Eu Helical System. Inorganic Chemistry, 2009, 48, 6341-6343.	1.9	74
24	Assembly of a Series of Trinuclear Zinc(II) Compounds with N ₂ O ₂ Donor Tetradentate Symmetrical Schiff Base Ligand. Crystal Growth and Design, 2010, 10, 4014-4022.	1.4	72
25	Metal-directed assembly of two 2-D 4d–4f coordination polymers based on elliptical triple-deck cylinders hinged by meso-double helical chains. CrystEngComm, 2009, 11, 1006.	1.3	67
26	Conversion of nonporous helical cadmium organic framework to a porous form. Chemical Communications, 2010, 46, 5373.	2.2	66
27	Oxygen Vacancy-Rich Mixed-Valence Cerium MOF: An Efficient Separator Coating to High-Performance Lithium–Sulfur Batteries. ACS Applied Materials & Interfaces, 2021, 13, 3899-3910.	4.0	65
28	Self-assembly of silver(I) polymers with single strand double-helical structures containing the ligand O,O′-bis(8-quinolyl)-1,8-dioxaoctane. Dalton Transactions RSC, 2001, , 2429-2434.	2.3	60
29	Mesoporous Mn ₃ O ₄ /C Microspheres Fabricated from MOF Template as Advanced Lithium-Ion Battery Anode. Crystal Growth and Design, 2017, 17, 5881-5886.	1.4	60
30	Controllable Synthesis of COFsâ€Based Multicomponent Nanocomposites from Coreâ€Shell to Yolkâ€Shell and Hollowâ€Sphere Structure for Artificial Photosynthesis. Advanced Materials, 2021, 33, e2105002.	11.1	60
31	Self-Assembly of Two Novel Cadmium(II) Complexes: One from Tripodal Imineâ^'Phenol Ligand and the Other from In situ Partial Degradation of Dipolar Imineâ^'Phenol Ligand. Crystal Growth and Design, 2008, 8, 2076-2079.	1.4	59
32	Coordination-directed assembly of trigonal and tetragonal molecular boxes encapsulating anionic guests â€. Dalton Transactions RSC, 2001, , 359-361.	2.3	58
33	Formation of Nâ€Doped Carbonâ€Coated ZnO/ZnCo ₂ O ₄ /CuCo ₂ O ₄ Derived from a Polymetallic Metal–Organic Framework: Toward Highâ€Rate and Longâ€Cycleâ€Life Lithium Storage. Small, 2017, 13, 1702150.	5.2	58
34	Construction of a Novel Znâ~'Ni Trinuclear Schiff Base and a Ni ²⁺ Chemosensor. Inorganic Chemistry, 2010, 49, 7241-7243.	1.9	57
35	Temperature- and solvent-controlled dimensionality in a zinc 6-(1H-benzoimidazol-2-yl)pyridinecarboxylate system. CrystEngComm, 2009, 11, 847.	1.3	55
36	Covalent Organic Frameworks as the Coating Layer of Ceramic Separator for High-Efficiency Lithium–Sulfur Batteries. ACS Applied Nano Materials, 2018, 1, 132-138.	2.4	55

#	Article	IF	CITATIONS
37	ZnO-based microrockets with light-enhanced propulsion. Nanoscale, 2017, 9, 15027-15032.	2.8	53
38	Mesoporous MnO/C–N Nanostructures Derived from a Metal–Organic Framework as High-Performance Anode for Lithium-Ion Battery. Inorganic Chemistry, 2017, 56, 9966-9972.	1.9	52
39	Formation of Racemate and Mesocate Complexes from an Achiral Tripodal Ligand Containing Three Benzimidazole Groups. Inorganic Chemistry, 2003, 42, 163-168.	1.9	51
40	Asymmetric Michael Addition of Oxindoles to Allenoate Catalyzed by <i>N</i> â€Acyl Aminophosphine: Construction of Functionalized Oxindoles with Quaternary Stereogenic Center. Advanced Synthesis and Catalysis, 2014, 356, 359-363.	2.1	51
41	Bifunctional 2D Cd(II)-Based Metal–Organic Framework as Efficient Heterogeneous Catalyst for the Formation of C–C Bond. Crystal Growth and Design, 2018, 18, 2883-2889.	1.4	51
42	Pillar-Layered Metal–Organic Framework with Sieving Effect and Pore Space Partition for Effective Separation of Mixed Gas C ₂ H ₂ /C ₂ H ₄ . ACS Applied Materials & Interfaces, 2017, 9, 29374-29379.	4.0	50
43	Understanding of Imine Substitution in Wide-Bandgap Polymer Donor-Induced Efficiency Enhancement in All-Polymer Solar Cells. Chemistry of Materials, 2019, 31, 8533-8542.	3.2	49
44	Construction of Low-Dimensional Cadmium Compounds with N ₂ O/N ₂ S Donor Tridentate Schiff Base Ligands. Crystal Growth and Design, 2009, 9, 3776-3788.	1.4	48
45	Lithium bis(trifluoromethanesulfonyl)imide assisted dual-functional separator coating materials based on covalent organic frameworks for high-performance lithium–selenium sulfide batteries. Journal of Materials Chemistry A, 2019, 7, 16323-16329.	5.2	48
46	Efficient Charge Migration in Chemically-Bonded Prussian Blue Analogue/CdS with Beaded Structure for Photocatalytic H ₂ Evolution. Jacs Au, 2021, 1, 212-220.	3.6	47
47	Partially cyclopentadienyl-substituted tetranuclear lanthanide Schiff base complexes. Journal of Organometallic Chemistry, 2001, 628, 99-106.	0.8	45
48	3D pillar-layered 4d–4f heterometallic coordination polymers based on pyridine-3,5-dicaboxylate and oxalate mixed ligands. Inorganic Chemistry Communication, 2009, 12, 316-320.	1.8	44
49	Sulfophilic and lithophilic sites in bimetal nickel-zinc carbide with fast conversion of polysulfides for high-rate Li-S battery. Chemical Engineering Journal, 2021, 404, 126566.	6.6	44
50	Construction of four 3d–4f heterometallic pillar-layered frameworks containing left- and right-handed helical chains and a I ^{â^'} chemosensor. CrystEngComm, 2015, 17, 3945-3952.	1.3	42
51	Steerable light-driven TiO2-Fe Janus micromotor. Inorganic Chemistry Communication, 2018, 91, 1-4.	1.8	42
52	Novel honeycomb silicon wrapped in reduced graphene oxide/CNT system as high-stability anodes for lithium-ion batteries. Electrochimica Acta, 2019, 317, 583-593.	2.6	42
53	One body, two hands: photocatalytic function- and Fenton effect-integrated light-driven micromotors for pollutant degradation. Nanoscale, 2019, 11, 16592-16598.	2.8	41
54	Synthesis, crystal structures and photoluminescence of Zn–Ln heterometallic polymers based on pyridine-2,3-dicarboxylic acid. Inorganic Chemistry Communication, 2009, 12, 761-765.	1.8	40

#	Article	IF	CITATIONS
55	Impact of Donor–Acceptor Interaction and Solvent Additive on the Vertical Composition Distribution of Bulk Heterojunction Polymer Solar Cells. ACS Applied Materials & Interfaces, 2019, 11, 45979-45990.	4.0	40
56	Rational Electrolyte Design to Form Inorganic–Polymeric Interphase on Silicon-Based Anodes. ACS Energy Letters, 2021, 6, 1811-1820.	8.8	39
57	Syntheses and characterization of copper(II) complexes of bis(acetylacetone)trimethylenediimine. Polyhedron, 2001, 20, 657-662.	1.0	37
58	Construction of three one-dimensional zinc(II) complexes containing pyrazine-2,3-dicarboxylic acid. Inorganica Chimica Acta, 2009, 362, 2619-2626.	1.2	37
59	Syntheses and characterizations of two lanthanide(III)–copper(II) coordination polymers constructed by pyridine-2,6-dicarboxylic acid. Inorganica Chimica Acta, 2005, 358, 1298-1304.	1.2	34
60	Construction of four 3d-4d/4d complexes based on salen-type schiff base ligands. CrystEngComm, 2011, 13, 6911.	1.3	34
61	Highly enantioselective synthesis of α-fluoro-α-nitro esters via organocatalyzed asymmetric Michael addition. Tetrahedron, 2011, 67, 312-317.	1.0	34
62	Novel bread-like nitrogen-doped carbon anchored nano-silicon as high-stable anode for lithium-ion batteries. Applied Surface Science, 2020, 511, 145609.	3.1	34
63	Three-Dimensional (3D) Nanostructured Skeleton Substrate Composed of Hollow Carbon Fiber/Carbon Nanosheet/ZnO for Stable Lithium Anode. ACS Applied Materials & Interfaces, 2021, 13, 3078-3088.	4.0	34
64	Metal–Organic Frameworks with Achiral/Monochiral Nano-Channels. Crystal Growth and Design, 2011, 11, 2824-2828.	1.4	33
65	<i>In situ</i> synthesis of Cu ₂ O–CuO–C supported on copper foam as a superior binder-free anode for long-cycle lithium-ion batteries. Materials Chemistry Frontiers, 2018, 2, 2254-2262.	3.2	33
66	Bithieno[3,4-c]pyrrole-4,6-dione-Mediated Crystallinity in Large-Bandgap Polymer Donors Directs Charge Transportation and Recombination in Efficient Nonfullerene Polymer Solar Cells. ACS Energy Letters, 2020, 5, 367-375.	8.8	33
67	Porous carbon with large surface area derived from a metal–organic framework as a lithium-ion battery anode material. RSC Advances, 2017, 7, 34104-34109.	1.7	32
68	Mesoporous spindle-like hollow CuO/C fabricated from a Cu-based metal-organic framework as anodes for high-performance lithium storage. Journal of Alloys and Compounds, 2017, 727, 1020-1026.	2.8	31
69	Iron Carbide Dispersed on Nitrogen-Doped Graphene-like Carbon Nanosheets for Fast Conversion of Polysulfides in Li–S Batteries. ACS Applied Nano Materials, 2020, 3, 9686-9693.	2.4	31
70	Two low-dimensional Schiff base copper(<scp>i</scp> ii) complexes: synthesis, characterization and catalytic activity for degradation of organic dyes. CrystEngComm, 2014, 16, 7926.	1.3	30
71	Three-fold parallel interlocking of 2-D brick-wall networks showing ladder-like unsymmetrical Borromean links. CrystEngComm, 2006, 8, 827.	1.3	29
72	Synthesis, crystal structures and properties of Ln(iii)–Cu(i)–Na(i) and Ln(iii)–Ag(i) heterometallic coordination polymers. CrystEngComm, 2011, 13, 3910.	1.3	29

#	Article	IF	CITATIONS
73	Construction of three high-dimensional supramolecular networks from temperature-driven conformational isomers. CrystEngComm, 2011, 13, 67-71.	1.3	29
74	Temperature-/solvent-dependent low-dimensional compounds based on quinoline-2,3-dicarboxylic acid: Structures and fluorescent properties. Dalton Transactions, 2012, 41, 11898.	1.6	29
75	Efficient removal of low-concentration organoarsenic by Zr-based metal–organic frameworks: cooperation of defects and hydrogen bonds. Environmental Science: Nano, 2019, 6, 3590-3600.	2.2	29
76	Oneâ€, Two―and Threeâ€Dimensional 3dâ€4f Heterometal Complexes Constructed from Pyridineâ€2,3â€dicarboxylic Acid. European Journal of Inorganic Chemistry, 2012, 2012, 5562-5570.	1.0	27
77	Highly efficient visible-light-driven oxygen-vacancy-based Cu ₂₊₁ O micromotors with biocompatible fuels. Nanoscale Horizons, 2020, 5, 325-330.	4.1	27
78	A series of lanthanide complexes based on pyridine-3,5-dicarboxylate and succinate ligands: syntheses, structures and properties. CrystEngComm, 2014, 16, 6797.	1.3	26
79	Auxiliary Ligand-Dependent Assembly of Several Ni/Niâ~'Cd Compounds with N ₂ O ₂ Donor Tetradentate Symmetrical Schiff Base Ligand. Crystal Growth and Design, 2010, 10, 4987-4994.	1.4	25
80	Trimetallic MOF-Derived Cu _{0.39} Zn _{0.14} Co _{2.47} O ₄ –CuO Interwoven with Carbon Nanotubes on Copper Foam for Superior Lithium Storage with Boosted Kinetics. ACS Sustainable Chemistry and Engineering, 2019, 7, 15684-15695.	3.2	25
81	Saclike-silicon nanoparticles anchored in ZIF-8 derived spongy matrix as high-performance anode for lithium-ion batteries. Journal of Colloid and Interface Science, 2020, 565, 315-325.	5.0	25
82	Syntheses and characterization of the samarium(III)–copper(II) 3D coordination network constructed by iminodiacetic acid. Journal of Solid State Chemistry, 2005, 178, 3729-3734.	1.4	23
83	Construction of three low dimensional Zn(II) complexes based on different organic-carboxylic acids. Inorganica Chimica Acta, 2009, 362, 1441-1447.	1.2	23
84	Syntheses and conversions of dinuclear cadmium(ii) compounds containing N2O/N2O2 donor tridentate/tetradentate asymmetrical Schiff base ligands. CrystEngComm, 2010, 12, 4012.	1.3	23
85	Temperature-induced two copper (II) supramolecular isomers constructed from 2-ethyl-1H-imidazole-4, 5-dicarboxlylate. Inorganic Chemistry Communication, 2011, 14, 1479-1484.	1.8	23
86	Two Schiff base ligands for distinguishing Zn ^{II} /Cd ^{II} sensing—effect of substituent on fluorescent sensing. RSC Advances, 2015, 5, 27682-27689.	1.7	23
87	Four metal–organic frameworks based on a semirigid tripodal ligand and different secondary building units: structures and electrochemical performance. CrystEngComm, 2016, 18, 6841-6848.	1.3	23
88	Synthesis and characterization of zinc(II) and cobalt(III) Schiff base complexes. Transition Metal Chemistry, 2009, 34, 115-120.	0.7	22
89	Covalent Organic Framework Based Functional Materials: Important Catalysts for Efficient CO ₂ Utilization. Angewandte Chemie, 2022, 134, .	1.6	22
90	Synthesis and spectroscopic studies of the cobalt(II) complex with methyl 2-pyridylmethylidenehydrazinecarbodithioate (HNNS). Transition Metal Chemistry, 2007, 32, 338-343.	0.7	21

#	Article	IF	CITATIONS
91	Construction of variable dimensional cadmium(<scp>ii</scp>) coordination polymers from pyridine-2,3-dicarboxylic acid. CrystEngComm, 2015, 17, 3619-3626.	1.3	21
92	A Molecular Chameleon with Fluorescein and Rhodamine Spectroscopic Behaviors. Inorganic Chemistry, 2016, 55, 205-213.	1.9	21
93	A Versatile Anionic Cd(II)-Based Metal–Organic Framework for CO ₂ Capture and Nitroaromatic Explosives Detection. Crystal Growth and Design, 2018, 18, 7088-7093.	1.4	21
94	CuCo ₂ S ₄ Nanosheets Coupled With Carbon Nanotube Heterostructures for Highly Efficient Capacitive Energy Storage. ChemElectroChem, 2018, 5, 2496-2502.	1.7	21
95	Quantitative Determination of the Vertical Segregation and Molecular Ordering of PBDB-T/ITIC Blend Films with Solvent Additives. ACS Applied Materials & Interfaces, 2020, 12, 24165-24173.	4.0	21
96	A non-interpenetrating 2D coordination polymer from a (CH2)8 spacer-based highly flexible linear ligand and AgCF3CO2Electronic supplementary information (ESI) available: 1H NMR spectra and data for C8TQ and complex 1 and the 3-D structure of complex 1. See http://www.rsc.org/suppdata/nj/b3/b301777j. New Journal of Chemistry, 2003, 27, 790-792.	1.4	20
97	From Metal–Organic Framework to Porous Carbon Polyhedron: Toward Highly Reversible Lithium Storage. Inorganic Chemistry, 2017, 56, 10007-10012.	1.9	20
98	The Development of Catalyst Materials for the Advanced Lithium–Sulfur Battery. Catalysts, 2020, 10, 682.	1.6	20
99	Construction of three pH-dependent luminescent metal–organic frameworks with 3-(4-carboxyphen-yl)-1,3-benzoimidazole. CrystEngComm, 2014, 16, 3883.	1.3	19
100	Anion-Dependent Assembly of Four Sensitized Near-Infrared Luminescent Heteronuclear Zn ^{II} –Yb ^{III} Schiff Base Complexes from a Trinuclear Zn ^{II} Complex. Inorganic Chemistry, 2014, 53, 9625-9632.	1.9	19
101	Two series of Ln(<scp>iii</scp>)–Ag(<scp>i</scp>) heterometallic–organic frameworks constructed from isonicotinate and 2,2′-biphenyldicarboxylate: synthesis, structure and photoluminescence properties. CrystEngComm, 2015, 17, 3800-3808.	1.3	19
102	Rapid naked-eye luminescence detection of carbonate ion through acetonitrile hydrolysis induced europium complexes. CrystEngComm, 2018, 20, 7574-7581.	1.3	19
103	Synergistic Effects of Polymer Donor Backbone Fluorination and Nitrogenation Translate into Efficient Non-Fullerene Bulk-Heterojunction Polymer Solar Cells. ACS Applied Materials & Interfaces, 2020, 12, 9545-9554.	4.0	19
104	Hybrid Cobalt(II) Fluoride Derived from a Bimetallic Zeolitic Imidazolate Framework as a High-Performance Cathode for Lithium–Ion Batteries. Journal of Physical Chemistry C, 2020, 124, 8624-8632.	1.5	19
105	A 2D pillar-layered coordination framework with meso-helix constructed from imidazole-4,5-dicarboxlylate and terephthalate. Inorganic Chemistry Communication, 2010, 13, 1439-1444.	1.8	18
106	1-D to 3-D lanthanide coordination polymers constructed from 5-aminoisophthalic acid and oxalic acid. Inorganic Chemistry Communication, 2012, 23, 25-30.	1.8	18
107	Single-crystal to single-crystal transformation from a 1-D chain-like structure to a 2-D coordination polymer on heating. CrystEngComm, 2013, 15, 5606.	1.3	18
108	A robust porous pillar-chained Cd-framework with selective sorption for CO2 and guest-driven tunable luminescence. CrystEngComm, 2014, 16, 3848.	1.3	18

#	Article	IF	CITATIONS
109	One Modification, Two Functions: Single Niâ€modified Lightâ€Driven ZnO Microrockets with Both Efficient Propulsion and Steerable Motion. Chemistry - an Asian Journal, 2019, 14, 2485-2490.	1.7	18
110	A series of temperature-dependent Cd ^{II} -complexes containing an important family of N-rich heterocycles from in situ conversion of pyridine-type Schiff base. RSC Advances, 2015, 5, 27743-27751.	1.7	17
111	Nanoâ€Sized AlPO ₄ Coating Layer on Graphite Powder to Improve the Electrochemical Properties of Highâ€Voltage Graphite/LiNi _{0.5} Mn _{1.5} O ₄ Liâ€Ion Cells. Energy Technology, 2019, 7, 1801078.	1.8	17
112	Title is missing!. Transition Metal Chemistry, 2000, 25, 594-598.	0.7	15
113	Construction of one 2D samarium-organic framework based on 2,4′-biphenyldicarboxylate. Inorganic Chemistry Communication, 2011, 14, 458-462.	1.8	15
114	The first Mn–Zn heterometallic dinuclear compound based on Schiff base ligand N, N′-bis(salicylidene)-1,3-diaminopropane. Inorganic Chemistry Communication, 2011, 14, 1228-1232.	1.8	15
115	Metal cation-dependent construction of two 3-D interpenetrating networks based on the ligand 1-(4-carboxyphenyl)-1,2,4-triazole. Inorganic Chemistry Communication, 2014, 39, 70-74.	1.8	15
116	From 1D to 3D lanthanide coordination polymers constructed with pyridine-3,5-dicarboxylic acid: synthesis, crystal structures, and catalytic properties. RSC Advances, 2016, 6, 63425-63432.	1.7	15
117	Structural diversity of Mn(<scp>ii</scp>), Zn(<scp>ii</scp>) and Pb(<scp>ii</scp>) coordination polymers constructed from isomeric pyridylbenzoate N-oxide ligands: structures and electrochemical properties. CrystEngComm, 2016, 18, 9307-9315.	1.3	15
118	Dynamic self-assembly of micro-nanomotor. Inorganic Chemistry Communication, 2018, 91, 8-15.	1.8	15
119	Copper nanowires and copper foam multifunctional bridges in zeolitic imidazolate framework–derived anode material for superior lithium storage. Journal of Colloid and Interface Science, 2020, 565, 156-166.	5.0	15
120	A new 3D fluorescent lanthanide-organic framework containing helical chains and zigzag layers from mixed carboxylate ligands. Inorganic Chemistry Communication, 2011, 14, 68-71.	1.8	14
121	Two novel 3D microporous heterometallic 3d–4f coordination frameworks with unique (7,) Tj ETQq1 1 0.7843 Communication, 2012, 16, 95-99.	14 rgBT /0 1.8	Overlock 10 14
122	Carbonâ€Dotâ€Induced Acceleration of Lightâ€Driven Micromotors with Inherent Fluorescence. Advanced Intelligent Systems, 2020, 2, 1900159.	3.3	14
123	Adiponitrile (ADN): A Stabilizer for the LiNi _{0.8} Co _{0.1} Mn _{0.1} O ₂ (NCM811) Electrode/Electrolyte Interface of a Graphite/NCM811 Li-Ion Cell. ACS Applied Materials & Interfaces, 2022, 14, 11398-11407.	4.0	14
124	MOF-Derived Bimetal ZnPd Alloy as a Separator Coating with Fast Catalysis of Lithium Polysulfides for Li–S Batteries. ACS Applied Energy Materials, 2021, 4, 13183-13190.	2.5	13
125	Efficient synthesis of novel sixâ€member ringâ€fused quinoline derivatives via the friedläder reaction. Heteroatom Chemistry, 2008, 19, 229-233.	0.4	12
126	Syntheses and characterization of three lanthanide(III) complexes containing pyridine-3,5-dicarboxylic acid ligands. Journal of Coordination Chemistry, 2009, 62, 2796-2803.	0.8	12

#	Article	IF	CITATIONS
127	High doses of (â^')-epigallocatechin-3-gallate from green tea induces cardiac fibrosis in mice. Biotechnology Letters, 2015, 37, 2371-2377.	1.1	12
128	One new 2D cadmium-organic framework containing 2,4′-biphenyldicarboxylate ligand. Inorganic Chemistry Communication, 2011, 14, 247-250.	1.8	11
129	Effect of lanthanide contraction on structures of lanthanide coordination polymers based on 5-aminoisophthalic acid and oxalate. Inorganic Chemistry Communication, 2012, 23, 127-131.	1.8	11
130	A versatile Cu ^{II} /Cu ^I metal–organic framework for selective sorption and heterogeneous catalysis. CrystEngComm, 2015, 17, 6693-6698.	1.3	11
131	Two 2-D 4-connected lanthanide coordination framework based on benzimidazole-5,6-dicarboxylate and acetate mixed ligands. Inorganic Chemistry Communication, 2010, 13, 1580-1584.	1.8	10
132	Temperature-dependent assemblies from a 2-D triple-stranded meso-helical layer to a 3-D chain-layer metal–organic framework. Dalton Transactions, 2012, 41, 14239.	1.6	10
133	Construction of four low-dimensional NIR-luminescence-tunable Yb(<scp>iii</scp>) complexes. Dalton Transactions, 2014, 43, 14009.	1.6	10
134	Axial Cl/Br atom-mediated CO ₂ electroreduction performance in a stable porphyrin-based metal–organic framework. Chemical Communications, 2020, 56, 14817-14820.	2.2	10
135	Construction of Zn ^{II} â€based <i>rac</i> â€Helical Chains Containing Semiâ€rigid Dipolar Ligand 1,4â€Bis(benzimidazolâ€1â€ylmethyl)benzene. Zeitschrift Fur Anorganische Und Allgemeine Chemie, 2009, 635, 567-571.	0.6	9
136	2D pillar-chained 3d-4f heterometallic coordination polymers based on 2,4′-biphenyldicarboxylate. Inorganic Chemistry Communication, 2011, 14, 453-457.	1.8	9
137	Efficient synthesis and characterization of the low dimensional heteronuclear complexes with a N2O2-donor Schiff base ligand. Inorganica Chimica Acta, 2012, 392, 177-183.	1.2	9
138	Cd ^{II} -Mediated Efficient Synthesis and Complexation of Asymmetric Tetra-(2-pyridine)-Substituted Imidazolidine. Crystal Growth and Design, 2014, 14, 5339-5343.	1.4	9
139	Four new Zn(<scp>ii</scp>) and Cd(<scp>ii</scp>) coordination polymers using two amide-like aromatic multi-carboxylate ligands: synthesis, structures and lithium–selenium batteries application. RSC Advances, 2019, 9, 14750-14757.	1.7	9
140	Relationships between Structure, Composition, and Electrochemical Properties in LiNi _{<i>x</i>} Mn _{2–<i>x</i>} O ₄ [<i>x</i> = 0.37, 0.43, 0.49, 0.52, and 0.56] Spinel Cathodes for Lithium Ion Batteries. Journal of Physical Chemistry C, 2019, 123, 8522-8530.	1.5	9
141	Assemblies of several supramolecular networks containing quinoline-2,3-dicarboxylic acid. New Journal of Chemistry, 2013, 37, 933.	1.4	8
142	(â^')-Epicatechin-3-gallate (a polyphenol from green tea) potentiates doxorubicin-induced apoptosis in H9C2 cardiomyocytes. Biotechnology Letters, 2015, 37, 1937-1943.	1.1	8
143	A series of variable coordination polymers based on flexible aromatic carboxylates. CrystEngComm, 2015, 17, 1326-1335.	1.3	8
144	Effect of annealing time on properties of spinel LiNi0.5Mn1.5O4 high-voltage lithium-ion battery electrode materials prepared by co-precipitation method. Ionics, 2017, 23, 2275-2283.	1.2	8

#	Article	IF	CITATIONS
145	Method for Synthesis of Zeolitic Imidazolate Framework-Derived LiCoO ₂ /CNTs@AlF ₃ with Enhanced Lithium Storage Capacity. Inorganic Chemistry, 2019, 58, 11993-11996.	1.9	8
146	Acrylate-Substituted Thiadiazoloquinoxaline Yields Ultralow Band Gap (0.56 eV) Conjugated Polymers for Efficient Photoacoustic Imaging. ACS Applied Polymer Materials, 2021, 3, 3247-3253.	2.0	8
147	Vertical Distribution in Inverted Nonfullerene Polymer Solar Cells by Layerâ€by‣ayer Solution Fabrication Process. Physica Status Solidi - Rapid Research Letters, 2021, 15, 2100386.	1.2	8
148	Tuning the Metal Ions of Prussian Blue Analogues in Separators to Enable High-Power Lithium Metal Batteries. Nano Letters, 2022, 22, 4861-4869.	4.5	8
149	Spontaneous resolution of chiral bis-sulfoxides with asymmetric atropisomerism. CrystEngComm, 2014, 16, 3839-3842.	1.3	7
150	Two kinds of 3D coordination frameworks from monometallic to 4d–4f heterometallic: Synthesis, crystal structures, photoluminescence and magnetic properties. Inorganic Chemistry Communication, 2014, 46, 163-171.	1.8	7
151	Crystal structures and luminescent properties modulated by auxiliary ligands for series of lanthanide coordination polymers with triazole-benzoic acid. Inorganic Chemistry Communication, 2016, 71, 1-4.	1.8	7
152	Achiral aromatic solvent-induced assembly of 3-D homochiral porous 3d–4f heterometallic-organic frameworks based on isonicotinic acid. CrystEngComm, 2017, 19, 5956-5959.	1.3	7
153	Pronounced Dependence of Allâ€Polymer Solar Cells Photovoltaic Performance on the Alkyl Substituent Patterns in Large Bandgap Polymer Donors. ChemPhysChem, 2020, 21, 908-915.	1.0	7
154	A New Ester‣ubstituted Quinoxalineâ€Based Narrow Bandgap Polymer Donor for Organic Solar Cells. Macromolecular Rapid Communications, 2021, 42, e2000683.	2.0	7
155	Formation and conversion of six temperature-dependent fluorescent Zn ^{II} -complexes containing two in situ formed N-rich heterocyclic ligands. RSC Advances, 2017, 7, 6994-7002.	1.7	6
156	Hydrothermal synthesis of mesoporous SnO2 as a stabilized anode material of lithium-ion batteries. Ionics, 2019, 25, 5745-5757.	1.2	6
157	3D Heterometallic 3d–4f coordination polymers based on organodisulfonate ligand with isonicotinic acid as a co-ligand: synthesis, crystal structures, photoluminescent and magnetic properties. Journal of Coordination Chemistry, 2015, 68, 1776-1787.	0.8	5
158	Two samarium(iii) complexes with tunable fluorescence from in situ reactions of 2-ethoxy-6-((pyridin-2-ylmethylimino)methyl)phenol with Sm3+ ion. RSC Advances, 2016, 6, 94687-94691.	1.7	5
159	Mechanism of a Lithiated Interlayer for Improving the Cycle Life of High Voltage Li-Ion Batteries Using a Commercial Carbonate Electrolyte. Journal of Physical Chemistry C, 2020, 124, 8057-8066.	1.5	5
160	Rapid and Specific Enhanced Luminescent Switch of Aniline Gas by MOFs Assembled from a Planar Binuclear Cadmium(II) Metalloligand. Inorganic Chemistry, 2022, 61, 10844-10851.	1.9	5
161	Construction of one 2-D pillared-chained dysprosium-organic framework based on 3,4-quinolinedicarboxylic acid. Inorganic Chemistry Communication, 2012, 21, 8-11.	1.8	4
162	Construction of two 2-D lanthanide(III)-frameworks with triple-stranded double-helical character based on ligand 4-(benzimidazol-1-ylmethyl)benzoate. Inorganic Chemistry Communication, 2013, 38, 65-69.	1.8	4

#	Article	IF	CITATIONS
163	Compatible Acceptors Mediate Morphology and Charge Generation, Transpration, Extraction, and Energy Loss in Efficient Ternary Polymer Solar Cells. ACS Applied Energy Materials, 2021, 4, 10187-10196.	2.5	4
164	Single-Metal Hybrid Micromotor. Frontiers in Bioengineering and Biotechnology, 2022, 10, 844328.	2.0	4
165	Synthesis and characterization of two temperature-dependent copper(II) complexes based on 2,6-dimethylpyridine-3,5-dicarboxylate. Journal of Coordination Chemistry, 2009, 62, 2480-2489.	0.8	3
166	Highly Specific Probe for Ferric Ions in Aqueous Solution Based on 5, 6â€Dicarboxyâ€3 <i>H</i> â€benzoimidazolâ€1â€ium Nitrate. Zeitschrift Fur Anorganische Und Allgemeine Chem 2014, 640, 1494-1498.	iep.6	3
167	Metal cation-dependent helicity of two 1-D heterometal chains constructed from pyridine-2,6-dicarboxylate. Inorganic Chemistry Communication, 2016, 73, 52-56.	1.8	3
168	In situ construction of two substituent-related dinuclear zinc(II) azaheterocyclic complexes from two simple Schiff base ligands with pyridyl terminal groups. Inorganic Chemistry Communication, 2017, 77, 59-63.	1.8	3
169	Synthesis of a Eu complex based on benzonitrile hydrolysis as the first luminescent probe for clinafloxacin. CrystEngComm, 2021, 23, 3602-3608.	1.3	3
170	Syntheses, structures and luminescence of a series of 4d–4f heterometallic coordination polymers constructed by 4,4′-oxybis(benzoicacid). Inorganic Chemistry Communication, 2013, 35, 217-220.	1.8	2
171	One-Step Hydrothermal Synthesis of SnO2@Carbon Composites with Super Lithium Ions Storage Performances. Journal of Nanoscience and Nanotechnology, 2019, 19, 4556-4564.	0.9	2
172	Synthesis and Characterization of Bis(methyl-2-pyridylmethylidenedrazinecarbodithioate)manganese(II). Journal of Chemical Crystallography, 2008, 38, 845-849.	0.5	1
173	Bis[methyl 2-(2-pyridylmethylidene)hydrazinecarbodithioato]zinc(II). Acta Crystallographica Section E: Structure Reports Online, 2008, 64, m328-m329.	0.2	0